J. Fluid Mech. (2014), *vol.* 746, *pp.* 99–122.
doi:10.1017/jfm.2014.98

New scaling laws for turbulent Poiseuille flow with wall transpiration

V. Avsarkisov[1,†], M. Oberlack[1,2,3,†] and S. Hoyas[4,‡]

[1]Chair of Fluid Dynamics, TU Darmstadt, Otto-Berndt-Strasse 2, 64287 Darmstadt, Germany

[2]Centre of Smart Interfaces, TU Darmstadt, Alarich-Weiss-Strasse 10, 64287 Darmstadt, Germany

[3]GS Computational Engineering, TU Darmstadt, Dolivostrasse 15, 64293 Darmstadt, Germany

[4]CMT Motores Térmicos, Universitat Politècnica de València, València, Spain

(Received 21 April 2013; revised 23 January 2014; accepted 18 February 2014;
first published online 28 March 2014)

A fully developed, turbulent Poiseuille flow with wall transpiration, i.e. uniform blowing and suction on the lower and upper walls correspondingly, is investigated by both direct numerical simulation (DNS) of the three-dimensional, incompressible Navier–Stokes equations and Lie symmetry analysis. The latter is used to find symmetry transformations and in turn to derive invariant solutions of the set of two- and multi-point correlation equations. We show that the transpiration velocity is a symmetry breaking which implies a logarithmic scaling law in the core of the channel. DNS validates this result of Lie symmetry analysis and hence aids establishing a new logarithmic law of deficit type. The region of validity of the new logarithmic law is very different from the usual near-wall log law and the slope constant in the core region differs from the von Kármán constant and is equal to 0.3. Further, extended forms of the linear viscous sublayer law and the near-wall log law are also derived, which, as a particular case, include these laws for the classical non-transpiring case. The viscous sublayer at the suction side has an asymptotic suction profile. The thickness of the sublayer increase at high Reynolds and transpiration numbers. For the near-wall log law we see an indication that it appears at the moderate transpiration rates ($0.05 < v_0/u_\tau < 0.1$) and only at the blowing wall. Finally, from the DNS data we establish a relation between the friction velocity u_τ and the transpiration v_0 which turns out to be linear at moderate transpiration rates.

Key words: turbulence simulation, turbulence theory

1. Introduction

In this paper we investigate the mean velocity scaling laws for a turbulent Poiseuille flow with uniform wall transpiration as it is shown in figure 1. Wall-bounded turbulent flows with transpiration may not only be a technologically important subject of investigation (Jiménez *et al.* 2001; Kametani & Fukagata 2011) but also important for theoretical reasons as we will subsequently show.

† Email addresses for correspondence: v.avsarkisov@astro-ge.org, oberlack@fdy.tu-darmstadt.de

‡ The original version of this article was published with the incorrect affiliation for S. Hoyas. A notice detailing this has been published online and in print, and the error rectified in the online PDF and HTML copies.

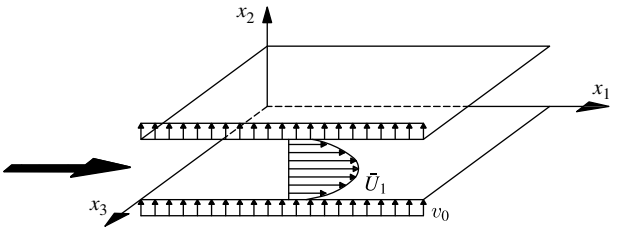

FIGURE 1. Schematic view of the channel flow with wall transpiration. Fluid is blown through the lower wall and removed from the upper wall at a constant rate.

In the classical non-transpiring plane turbulent channel flow all statistical quantities are symmetric or antisymmetric with respect to the channel centreline. This includes symmetric distribution of the mean velocity, the normal Reynolds stresses and point symmetric distributions of viscous and turbulent shear stresses including values of shear stresses at the walls. These results are consistent with zero total shear stress and zero mean velocity gradient in the centre of the channel. In the presence of wall transpiration, all of these symmetries are broken. Furthermore, the occurrence of an additional term in the streamwise component of the mean momentum equation modifies the classical universal scaling laws (linear viscous sublayer and law of the wall) for non-transpiring wall-bounded flows.

Boundary-layer flows with wall-transpiration are the most commonly studied wall-bounded flow with permeable boundary conditions. First experimental results and a new mean velocity scaling law (so-called 'bi-logarithmic law') on the subject were obtained in the 1950s (Mickley & Davis 1957; Black & Sarnecki 1958) using mixing-length theory. Tennekes (1965) obtained a new form of the law of the wall ('semi-logarithmic') and a velocity defect law assuming the existence of a joint velocity scale u_τ^2/v_0 for the inner and the outer regions. Later Stevenson in his two companion papers (Stevenson 1963*a*,*b*) compared his experimental results with the experimental data of Black & Sarnecki (1958) and Mickley & Davis (1957). He found generalized forms of the law of the wall and shortly afterwards a velocity defect law for the turbulent boundary layer with suction and blowing at zero pressure gradient. He stated that the slope constant, i.e. the von Kármán constant, and the additive constant C are both independent of the transpiration velocity v_0. The most recent study on turbulent boundary-layer flow with transpiration is a numerical one conducted by Schlatter & Örlü (2011). They showed that uniform suction considerably changes the mean velocity profile and they found the modified coefficients for the log law to be $\kappa = 0.82$ and $C = 9.2$.

In comparison with the other wall-bounded flows with specific, non-standard boundary conditions, turbulent channel, i.e. Poiseuille flow with wall transpiration is a relatively new subject of investigation. The only experimental study of this flow of an incompressible fluid known to the authors was conducted by Zhapbasbayev & Isakhanova (1998). They collected statistics for the mean velocity and turbulent stresses for different Reynolds numbers and a variety of small transpiration velocity numbers in the range $0 < v_0/u_\tau < 0.05$. Thereafter, they employed the experimental data to evaluate a Reynolds stress transport model developed by Launder and co-authors (see e.g. Hanjalić & Launder 1972*b*; Launder, Reece & Rodi 1975).

In the literature only a few direct numerical simulation (DNS) studies of the turbulent channel flow with blowing and suction were reported. Sumitani & Kasagi

(1995) studied turbulent channel flow with uniform wall transpiration and heat transfer. The walls were kept isothermal, while their temperatures vary. The Reynolds number and the transpiration rate were held constant at $Re_\tau = 150$ and $v_0/u_\tau = 0.05$. Various statistical quantities including mean velocity and mean temperature, Reynolds stresses and turbulent heat fluxes were obtained. Energy budgets and temperature correlations were also calculated. One key overall result they found was that blowing stimulates the near-wall turbulence and creates an excessive amount of small-scale coherent streamwise vortical structures, while suction suppresses turbulence and at the same time creates large-scale near-wall coherent structures. Nikitin & Pavel'ev (1998) performed DNS computations at $Re_\tau = 356$ and 681.2 for $v_0/u_\tau = 0.112$ and 0.118, respectively. They showed that blowing and suction increase the friction coefficient. Apart from this, they investigated the near-wall logarithmic region of the mean velocity profile and found that the slope constant of the log law at the blowing wall is not constant and increases with the increase of transpiration rate. It is important to mention that they used the local friction velocity at each wall as the velocity scale. Presently we employ an averaged friction velocity from both walls, which is a measure of the pressure gradient. Chung & Sung (2001) investigated the initial relaxation of a turbulent channel flow after a sudden application of blowing and suction. Chung, Sung & Krogstad (2002) analysed the effects of uniform wall blowing and suction by modulating the near-wall turbulence. They confirmed that suction increases the turbulence anisotropy, while blowing decreases the anisotropy in the near-wall region and enhances the transverse components of the velocity fluctuations (u_2 and u_3).

A purely analytical study of the turbulent channel flow with wall transpiration was performed by Vigdorovich & Oberlack (2008). Employing the method of matched asymptotic expansions led them to the construction of the solutions for the near-wall regions (both blowing and suction) as well as for the core region of the flow. The results therein did not give any scaling for the mean velocity or the correlation functions but it allowed the relation between the wall shear stress, the Reynolds number and the transpiration velocity to be described by a function of one variable.

Summarizing all above-mentioned studies we conclude that there is no comprehensive investigation of the mean velocity scaling laws of the Poiseuille flow with uniform wall transpiration based on first principles. This difficulty may be traced back to the problem of determining an appropriate velocity scale as there are multiple including v_0, u_τ on both walls and U_B being the bulk velocity, as well as the proper choice of equations on which to base the analysis.

Presently, the application of Lie symmetry method to the two-point correlation (TPC) and multi-point correlation (MPC) equations is employed as the fundamental basis to find new mean velocity scaling laws as well as the proper scales on which it is based. The DNS facilitates the evaluation of the analytical results and finally allows us to establish a clear connection between the different velocity scales.

Symmetry analysis of a system of differential equations based on continuous transformation groups, i.e. Lie groups, was introduced by Sophus Lie in the nineteenth century to unify and extend various specialized methods for solving differential equations. The symmetry of a system of differential equations is a transformation that maps any solution to another solution of the system. The advantage of Lie group method, and in turn constructing symmetry transformations, is that they can be found using computational methods. Finding of the symmetry transformations of the TPC equations gives profound insight into the flow physics. Once the symmetries are derived, they can be used to achieve reduction or self-similarity in a general

sense of the TPC equations. This reduction is always associated with the decrease of the number of independent variables and finally leads to the desired turbulent scaling laws. Presently, the main goal is to find mean velocity scaling laws, but Lie symmetry method is also useful for finding of scaling laws of any higher-order statistical quantity.

In a series of papers Oberlack and co-authors (see Oberlack 2000, 2001; Oberlack & Rosteck 2010; Rosteck & Oberlack 2011) studied the turbulent channel and other canonical wall-bounded flows using Lie symmetry theory by investigating the infinite series of MPC equations. Thereof they derived a variety of classical and new scaling laws. It was shown that they are exact solutions of symmetry invariant type of the infinite-dimensional series of MPC equations. They have shown that turbulent scaling laws may be generated from first principle and that most of the classical and new symmetry invariant solutions are based on one or several of the newly discovered statistical symmetry groups (Oberlack & Rosteck 2010).

In this paper we propose new scaling laws for turbulent Poiseuille flows with wall transpiration including the canonical flow without transpiration as a particular case. In addition, we obtain a new logarithmic scaling law in the centre of the channel using Lie symmetry methods. The law is of defect type and covers up to 75 % of the channel depending on the turbulent Reynolds number Re_τ and the transpiration velocity v_0. In order to validate the new scaling laws and to study the interplay between Reynolds and transpiration number effects, various DNS of the channel flow at $Re_\tau = 250$, 480 and 850 and a wide range of the transpiration velocities v_0 are conducted.

Governing equations for the flow with wall transpiration are given in § 2. A new log law is derived in § 3 and also it is shown that transpiration generalizes the classical laws for the viscous sublayer and the overlap region. DNS verification of the new scaling law is presented in § 4. Discussion and conclusions are given in § 5.

2. Basic equations for the turbulent channel flow and DNS

The analysis presented below is based on the mean friction velocity defined as follows

$$u_\tau \equiv \sqrt{\frac{u_{\tau b}^2 + u_{\tau s}^2}{2}} = \sqrt{\frac{1}{\rho}\frac{|\tau_{wb}| + |\tau_{ws}|}{2}} = \sqrt{\frac{h}{\rho}\left|\frac{\partial \bar{P}}{\partial x_1}\right|}, \tag{2.1}$$

which is a measure of the pressure gradient and the local friction velocities are defined as

$$u_{\tau b} = \sqrt{\nu\left|\frac{\partial \bar{U}_1}{\partial x_2}\right|_b}, \quad u_{\tau s} = \sqrt{\nu\left|\frac{\partial \bar{U}_1}{\partial x_2}\right|_s}. \tag{2.2}$$

Here, $\bar{U}_1$ and $(\partial \bar{P}/\partial x_1)$ are the mean velocity and mean pressure gradient in streamwise direction, ν is the kinematic viscosity and h is the channel half-width. Here and subsequently subscripts b and s correspond to variables taken on the blowing and the suction side, respectively. For variables at the wall we use the subscript w and variables without blowing and suction are denoted by 0. Dimensionless variables in the near-wall scaling will have the superscript $+$:

$$x_i^+ = \frac{x_i u_\tau}{\nu}, \quad \bar{U}_i^+ = \frac{\bar{U}_i}{u_\tau}, \quad \overline{u_i u_k}^+ = \frac{\overline{u_i u_k}}{u_\tau^2}, \quad v_0^+ = \frac{v_0}{u_\tau}, \quad \tau^+ = \frac{\tau}{(|\tau_{wb}| + |\tau_{ws}|)/2}. \tag{2.3}$$

Note that here u_τ is the mean friction velocity, which is a global parameter. Specific differences on each wall and the corresponding differences in scaling will be discussed in §§ 3.2–3.4. We employ the channel half-width h as a core region length scaling parameter. The bulk mean velocity is defined as

$$U_B = \frac{1}{2h}\int_0^{2h} \bar{U}_1(x_2)\,\mathrm{d}x_2. \tag{2.4}$$

It is suitable to start the analysis with the Navier–Stokes equations written in Reynolds-averaged form. Throughout this paper we use the following notation. The statistically averaged quantities are denoted by an overbar, e.g. $\bar{U}_i$ and $\bar{P}$, whereas fluctuating quantities are denoted by a lowercase letters, e.g. u_i and p. The governing equations for an incompressible turbulent flow, i.e. continuity and mean-momentum equations, are

$$\frac{\partial \bar{U}_k}{\partial x_k} = 0, \tag{2.5}$$

$$\frac{\partial \bar{U}_i}{\partial t} + \bar{U}_k\frac{\partial \bar{U}_i}{\partial x_k} = -\frac{1}{\rho}\frac{\partial \bar{P}}{\partial x_i} + \nu\frac{\partial^2 \bar{U}_i}{\partial x_k \partial x_k} - \frac{\partial \overline{u_i u_k}}{\partial x_k}, \quad i = 1, 2, 3, \tag{2.6}$$

where $\bar{U}_i(x_i,\, t)$ and $\bar{P}(x_i,\, t)$ are the mean velocity and mean pressure, and $\overline{u_i u_k}$ is the Reynolds stress tensor. For the incompressible flow investigated, pressure can be normalized with the constant density as follows

$$\bar{P}^* = \frac{\bar{P}}{\rho}. \tag{2.7}$$

The asterisk will be omitted throughout the paper. For the present flow we have the following boundary condition (BC) at the wall

$$\bar{U}_i(x_1;\, x_2 = 0,\, 2h;\, x_3) = (0;\, v_0;\, 0)^{\mathrm{T}}. \tag{2.8}$$

Because of the periodic BC in the streamwise direction and general homogeneity in this direction, continuity leads to a constant wall-normal velocity across the channel height, i.e.

$$\bar{U}_2(x_2) = v_0. \tag{2.9}$$

As we employ the BC $U_i(x_1;\, x_2 = 0,\, 2h;\, x_3) = (0;\, v_0;\, 0)^{\mathrm{T}}$ for the DNS together with (2.8) it implies that all fluctuations vanish at the wall, i.e. $u_i = 0$. Therefore, all Reynolds stresses also vanish at the wall.

With this, we obtain the streamwise component of mean momentum equation for the steady state

$$v_0\frac{\mathrm{d}\bar{U}_1}{\mathrm{d}x_2} = -\frac{\mathrm{d}\bar{P}}{\mathrm{d}x_1} - \frac{\mathrm{d}\overline{u_1 u_2}}{\mathrm{d}x_2} + \nu\frac{\mathrm{d}^2\bar{U}_1}{\mathrm{d}x_2^2}. \tag{2.10}$$

As the pressure gradient is specified as a constant, equation (2.10) may be integrated once and rearranged to obtain

$$\tau(x_2) - v_0\bar{U}_1 = -\overline{u_1 u_2} + \nu\frac{\mathrm{d}\bar{U}_1}{\mathrm{d}x_2} - v_0\bar{U}_1 = x_2\frac{\mathrm{d}\bar{P}}{\mathrm{d}x_1} + c_1. \tag{2.11}$$

Here c_1 is a constant that in the canonical channel flow is defined as ρu_τ^2 (Tennekes & Lumley 1972). Due to different wall conditions of the channel flow with transpiration the wall shear stresses on the blowing and suction walls are different, which brought the necessity to use a local friction velocity in (2.11) rather than a global one.

Profiles of the viscous stress, the Reynolds stress and the convective momentum transport together with the total shear stress are presented and discussed later.

2.1. *The TPC equations*

The space and time correlation functions in the theory of turbulence was first introduced by Keller & Friedmann (1924). Various authors derived the complete system of two-point correlation equations (see e.g. Hinze 1959; McComb 1990), while Keller & Friedmann (1924) were also the first who closed it by writing the third moment via the second moment and the mean. Later it was found that higher-order correlations may indeed not be neglected and the infinite number of the MPC equations rather than TPC should be taken into account. A first derivation of the full MPC equation may have been derived in Oberlack (2000).

In order to comprehend the question why the TPC or MPC equations need to be employed at all for finding the turbulent scaling laws we may for a moment consider the case of decaying isotropic turbulence. Here, the one-point equation $\mathrm{d}k/\mathrm{d}t = -\varepsilon$ does not deliver any information that the kinetic energy k usually may decay according to a power law, if some transitional period has passed. However, the corresponding two-point equation, the von Kármán–Howarth equation (von Kármán & Howarth 1938), admits a similarity solution as was already shown in the original paper of von Kármán–Howarth and, probably unknown to the authors, is an implicit use of Lie symmetries. It delivers the power law decay for the turbulent kinetic energy and at the same time the algebraic growth of the integral length scale. Hence, transferring back to the present problem of a shear flow with transpiration we may conclude that the mean momentum equation (2.10) alone is not sufficient to rigourously derive the requested scaling property.

In the present section we only focus on the TPC equations in its most general form

$$\begin{aligned}&\frac{\bar{\mathrm{D}}R_{ij}}{\bar{\mathrm{D}}t} + R_{kj}\frac{\partial \bar{U}_i(\boldsymbol{x},t)}{\partial x_k} + R_{ik}\left.\frac{\partial \bar{U}_j(\boldsymbol{x},t)}{\partial x_k}\right|_{\boldsymbol{x}+\boldsymbol{r}} + \left[\bar{U}_k(\boldsymbol{x}+\boldsymbol{r},t) - \bar{U}_k(\boldsymbol{x},t)\right]\frac{\partial R_{ij}}{\partial r_k}\\ &\quad + \frac{\partial \overline{pu}_j}{\partial x_i} - \frac{\partial \overline{pu}_j}{\partial r_i} + \frac{\partial \overline{u_i p}}{\partial r_j} - \nu\left[\frac{\partial^2 R_{ij}}{\partial x_k \partial x_k} - 2\frac{\partial^2 R_{ij}}{\partial x_k \partial r_k} + 2\frac{\partial^2 R_{ij}}{\partial r_k \partial r_k}\right]\\ &+ \quad \frac{\partial R_{(ik)j}}{\partial x_k} - \frac{\partial}{\partial r_k}[R_{(ik)j} - R_{i(jk)}] = 0,\end{aligned} \tag{2.12}$$

without introducing any closure, where the second- and third-order correlation tensors are defined as

$$\begin{aligned}&R_{ij}(\boldsymbol{x},\boldsymbol{r};t) = \overline{u_i(\boldsymbol{x},t)u_j(\boldsymbol{x}+\boldsymbol{r},t)}, \quad \overline{pu}_j = \overline{p(\boldsymbol{x},t)u_j(\boldsymbol{x}+\boldsymbol{r},t)}, \quad \overline{u_i p} = \overline{u_i(\boldsymbol{x},t)p(\boldsymbol{x}+\boldsymbol{r},t)},\\ &R_{(ik)j}(\boldsymbol{x},\boldsymbol{r};t) = \overline{u_i(\boldsymbol{x},t)u_k(\boldsymbol{x},t)u_j(\boldsymbol{x}+\boldsymbol{r},t)}, \quad R_{i(jk)}(\boldsymbol{x},\boldsymbol{r};t) = \overline{u_i(\boldsymbol{x},t)u_j(\boldsymbol{x}+\boldsymbol{r},t)u_k(\boldsymbol{x}+\boldsymbol{r},t)}.\end{aligned} \tag{2.13}$$

and $\bar{\mathrm{D}}/\bar{\mathrm{D}}t = (\partial/\partial t + \bar{U}_k(\partial/\partial x_k))$ is the mean substantial derivative. Continuity equations for the TPC have the following form

$$\frac{\partial R_{ij}}{\partial x_i} - \frac{\partial R_{ij}}{\partial r_i} = 0, \quad \frac{\partial R_{ij}}{\partial r_j} = 0 \tag{2.14}$$

and

$$\frac{\partial \overline{pu}_i}{\partial r_i} = 0, \quad \frac{\partial \overline{u_j p}}{\partial x_j} - \frac{\partial \overline{u_j p}}{\partial r_j} = 0. \tag{2.15}$$

Equations for higher-order correlations have a rather similar form and may be taken from Oberlack (2000). In the present study Lie group analysis is used to find symmetry transformations and in turn self-similar solutions of the TPC equations. For the present flow the TPC equations (2.12) reduce to the following form

$$\begin{aligned} &\bar{U}_2 \frac{\partial R_{ij}}{\partial x_2} + R_{2j}\delta_{i1} \frac{\partial \bar{U}_1(x_2)}{\partial x_2} + R_{i2}\delta_{1j} \left.\frac{\partial \bar{U}_1(x_2)}{\partial x_2}\right|_{x_2+r_2} + \frac{\partial \overline{pu}_j}{\partial x_i} - \frac{\partial \overline{pu}_j}{\partial r_i} \\ &\quad + \frac{\partial \overline{u_i p}}{\partial r_j} + \left[\bar{U}_1(x_2 + r_2) - \bar{U}_1(x_2)\right] \frac{\partial R_{ij}}{\partial r_1} - \nu \left[\frac{\partial^2 R_{ij}}{\partial x_2 \partial x_2} - 2\frac{\partial^2 R_{ij}}{\partial x_2 \partial r_2} + 2\frac{\partial^2 R_{ij}}{\partial r_k \partial r_k}\right] \\ &\quad + \frac{\partial R_{(i2)j}}{\partial x_2} - \frac{\partial}{\partial r_k}[R_{(ik)j} - R_{i(jk)}] = 0, \end{aligned} \tag{2.16}$$

since $\bar{U}_i(x_2) = (\bar{U}_1(x_2), \bar{U}_2, 0)$ and, we recall, $\bar{U}_2 = v_0$.

In this context a natural question arises as to why it is sufficient to employ the mean momentum and the TPC equation for the subsequent Lie symmetry analysis without taking into account the entire infinite set of MPC equations. Here, the deeper reason rests on the fact that correlation equations have only a coupling to the direct neighbouring equation of the next higher tensor order. Hence, without giving a proof for this, it is sufficient to verify that the derived symmetries for a given correlation tensor order are consistent to the next higher order. For the present case which relies on relatively simple symmetries this may readily be verified.

2.2. *DNS of the channel flow with wall blowing and suction*

In order to verify the scaling laws to be obtained for the different regions of the flow in the sections to follow we conduct a number of DNS for different transpiration rates and Reynolds numbers.

For the present DNS we employ a numerical code developed at the School of Aeronautics, Technical University of Madrid (Hoyas & Jiménez 2006). The code solves the Navier–Stokes equations for an incompressible fluid in velocity–vorticity formulation (see e.g. Kim, Moin & Moser 1987). In the streamwise and spanwise directions (x_1, x_3) Fourier discretization is used. In the wall-normal direction (x_2), a seven-point compact finite difference scheme (Lele 1992) is applied. Full details of the numerical methods are given in Hoyas & Jiménez (2006). The DNS data of Sumitani & Kasagi (1995) are used for the validation of the code. Validation results are not shown in the present paper, as they were included in Avsarkisov, Oberlack & Khujadze (2011).

Production runs can be divided into three sets depending on the friction Reynolds number Re_τ. The first two simulation sets consists of four cases for different transpiration rates, while the highest-Reynolds-number simulation set consists of only two cases for small and medium transpiration numbers. A complete summary of the flow and the numerical parameters are given in table 1. Using the DNS and the experimental results of Sumitani & Kasagi (1995) and Antonia *et al.* (1986) we concluded that for the smaller-Reynolds-number simulations ($Re_\tau = 250$) it will be sufficient to use a $4\pi h \times 2h \times 2\pi h$ box. A validation of this assumption may be taken from figure 4, where the results for the two-point cross-correlation function

Re_τ	v_0^+	v_0/U_b	L_{x_1}/h	L_{x_3}/h	Δx_1^+	Δx_3^+	N_{x_1}	N_{x_2}	N_{x_3}	N_F	$u_\tau T/h$
250	0	0	4π	2π	4.1	6.1	768	251	256	48	100
250	0.05	0.003	4π	2π	4.1	6.1	768	251	256	161	150
250	0.1	0.0069	4π	2π	4.2	6.1	768	251	256	197	70
250	0.16	0.0164	4π	2π	4.2	6.2	768	251	256	161	120
250	0.26	0.05	4π	2π	4.2	6.2	768	251	256	136	150
480	0	0	8π	6π	15.3	11.7	768	385	768	95	31
480	0.05	0.003	8π	6π	15.6	11.7	768	385	768	226	41
480	0.1	0.0075	8π	6π	15.6	11.7	768	385	768	310	40
480	0.16	0.0164	8π	6π	15.7	11.8	768	385	768	212	25
480	0.26	0.049	8π	6π	15.8	11.8	768	385	768	214	30
850	0.05	0.0026	8π	6π	6.8	5.1	3072	471	3072	160	26
850	0.16	0.016	8π	6π	7	5.2	3072	471	3072	205	22

TABLE 1. Summary of the simulations. Here $v_0^+ = v_0/u_\tau$ is the transpiration rate. Here $L_{x_1}, L_{x_3}, \Delta x_1^+$ and Δx_3^+ are the periodic dimensions of the numerical box and the resolutions in streamwise and spanwise directions, respectively. Here N_{x_1}, N_{x_2} and N_{x_3} are numbers of collocation points in streamwise, wall-normal and spanwise directions, respectively. Here N_F is the number of accumulated statistical fields and T is the computational time spanned by those fields.

$R_{12}/\sqrt{(\overline{u_1 u_2})^2}$ for $Re_\tau = 250$, $v_0^+ = 0.16$ are shown. For higher Reynolds numbers we selected a box similar to the one that was used by del Álamo & Jiménez (2003), del Álamo *et al.* (2004) and Hoyas & Jiménez (2006). Due to an increased dissipation at the blowing side we had to use more grid points in wall-normal direction than it is usually taken in a classical channel flow DNS to keep the resolution of $\Delta x_2 = 1.8\eta$ approximately constant in terms of the local Kolmogorov length scale η.

3. New scaling laws of the turbulent channel flow with wall transpiration

As was mentioned in the introduction, the existence of the uniform transpiration implies an asymmetry not only for the mean velocity profile, but also for the distribution of the stresses. Blowing redistributes Reynolds shear stress into the core region. This effect is similar to the one that is observed in a turbulent Couette–Poiseuille flow, where the position at which $\tau(x_2) = 0$ is no longer in the centre of the channel in contrast to what is seen in a pure Poiseuille-type flow (see e.g. Nakabayashi, Kitoh & Katoh 2004). In addition, we observe that suction creates a very high wall-normal gradient of the streamwise velocity in the vicinity of the suction wall. With growing transpiration rate this asymmetry is amplified exhibiting an ever-increasing difference in physical properties between the canonical channel flow and the flow with transpiration, as may be taken from the figures 2 and 3. At moderate transpiration rates, i.e. $u_\tau/v_0 < 0.16$, in the vicinity of the blowing side the transpiration velocity produces extra Reynolds shear stress and suppresses the viscous stress, while the reverse is observed on the suction side. At high transpiration rates, i.e. $0.16 \leqslant v_0/u_\tau \leqslant 0.26$, the Reynolds shear stress vanishes on the suction side, while the viscous stress disappears on the blowing one, as can be taken from figures 2(*d*,*e*) and 3(*d*,*e*). The flow in the near-wall region is rather particular and very different from the classical Poiseuille flow as in this region the transpiration velocity is an

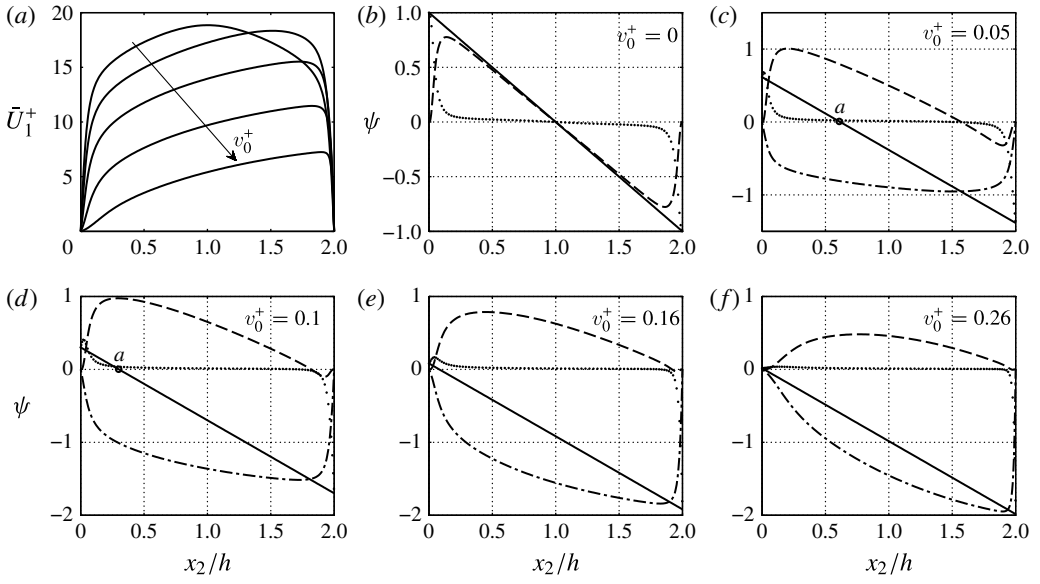

FIGURE 2. Mean velocity and shear stress distribution profiles at $Re_\tau = 250$ and $v_0^+ = 0.0$, 0.05, 0.1, 0.16 and 0.26. Panel (*a*) depicts mean velocity profiles and ψ in the panels (*b*)–(*f*) depict shear stress distributions with increasing transpiration rate: $\cdots$, $\mathrm{d}\bar{U}_1^+/\mathrm{d}x_2^+$; - - -, $\overline{u_1u_2}^+$; —, $\tau^+ - v_0^+\bar{U}_1^+$ $-\cdot-$, $v_0^+\bar{U}_1^+$. Blowing wall is at $x_2 = 0$ and suction wall is at $x_2 = 2h$. The point of zero shear stress measured from the blowing wall is denoted by *a*.

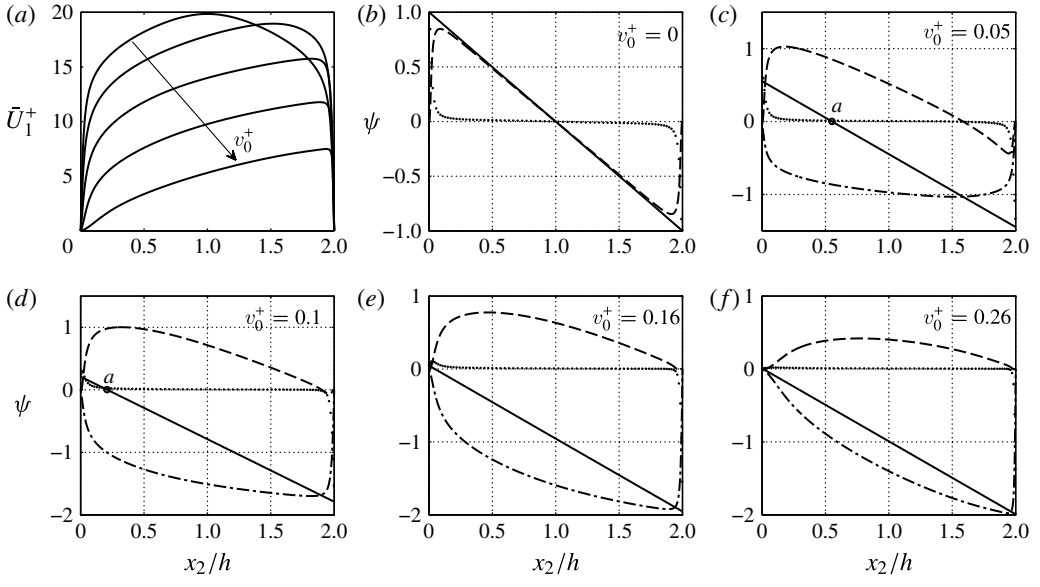

FIGURE 3. Mean velocity and shear stress distribution profiles at $Re_\tau = 480$ and $v_0^+ = 0.0$, 0.05, 0.1, 0.16 and 0.26. Panel (*a*) depicts mean velocity profiles and ψ in the panels (*b*)–(*f*) depict shear stress distributions with increasing transpiration rate: $\cdots$, $\mathrm{d}\bar{U}_1^+/\mathrm{d}x_2^+$; - - -, $\overline{u_1u_2}^+$; —, $\tau^+ - v_0^+\bar{U}_1^+$ $-\cdot-$, $v_0^+\bar{U}_1^+$. Blowing wall is at $x_2 = 0$ and suction wall is at $x_2 = 2h$. The point of zero shear stress measured from the blowing wall is denoted by *a*.

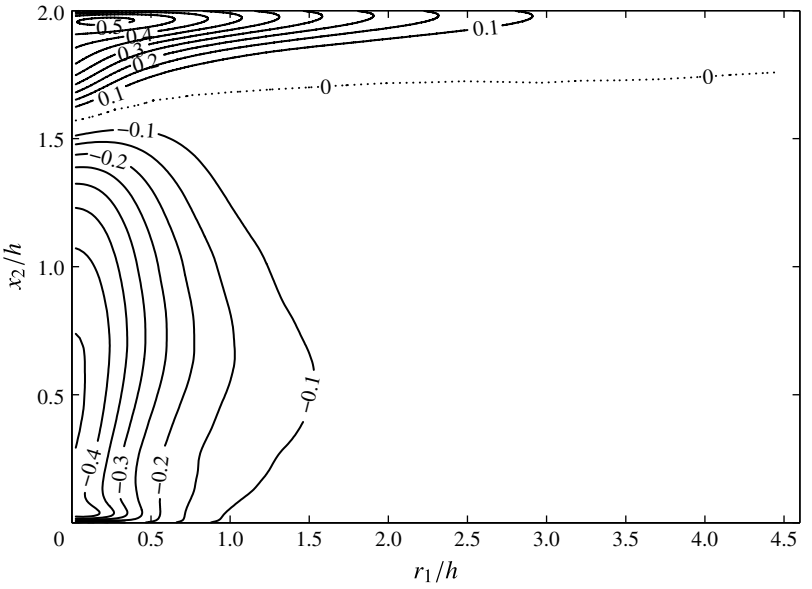

FIGURE 4. Isocontours of the two-point cross-correlation function normalized on stresses, i.e. $R_{12}/\sqrt{(\overline{u_1u_2})^2}$, as a function of the streamwise separation r_1/h and the wall-normal coordinate x_2/h: —, positive/negative; $\cdots$, zero. Further we have $r_2/h = r_3/h = 0$. The spacing of the contour lines is 0.05;

order of magnitude smaller than the streamwise velocity. As a result, in contrast to the classical flow, streamlines in the near-wall region are perpendicular to the wall. Further away from the wall they are strongly bent towards the downstream direction. A first theoretical attempt to study turbulent Poiseuille flow at high transpiration rates was made by Vigdorovich & Oberlack (2008), who used the method of matched asymptotic expansions to show that the skin friction vanishes at the blowing wall, while the point of maximum streamwise velocity approaches the suction wall.

A second critical effect, that can be taken from figures 2 and 3, is the non-coincidence of the points of zero turbulent shear stress with the point of zero viscous stress, which appears at high transpiration rates. Usually located in the centre of the channel, as is shown in figures 2(*b*) and 3(*b*), i.e. $x_2 = h$, the point of zero shear stress is slightly shifted towards the blowing wall while the point of maximum velocity moves towards the suction side.

The non-coincidence of the different locations of the two points with $\tau(x_2) = 0$ and $\bar{U}_{1max}(x_2)$ may not only be induced by transpiration. This effect, however, may also be observed in the turbulent channel flows with asymmetric boundary conditions such as, rough wall/smooth wall conditions (see e.g. Hanjalić & Launder 1972*a*) or, generally speaking, when the values of the stresses at the wall τ_w are different on the upper and the lower walls. The exception, when the difference of the stresses at the walls does not induce this non-coincidence of $\tau(x_2) = 0$ and $\bar{U}_{1max}(x_2)$ may be found in the Couette–Poiseuille flow, when there is no region of zero shear stress between the two walls (Couette-type flow) (see e.g. Nakabayashi *et al.* 2004; Johnstone, Coleman & Spalart 2010).

An interesting result was obtained from the analysis of the shear stress combined with the convective term, $\tau^+ - v_0^+ \bar{U}_1^+$. The point of the balance of shear stress

and convective momentum transport (a/h), approaches the blowing wall as the transpiration increases, that can be taken from the figures 2 and 3. From simple geometrical considerations one may derive the relation

$$\frac{a}{h} = \frac{\tau_{wb}}{(|\tau_{wb}| + |\tau_{ws}|)/2}, \tag{3.1}$$

which indicates that the position of the balance point depends on the values of the both shear stresses at the walls, i.e. τ_{wb} and τ_{ws}.

Another profound insight into the turbulence characteristics of the present flow type is obtained by analysing the TPCs. It may be taken from figure 4 that close to the suction wall ($x_2 \to 2h$) the streamwise two-point cross-correlation R_{12} indicates a rather long correlation length as it decays slowly in r_1 direction. In contrast, on the blowing side ($x_2 \to 0$) correlations show a considerably shorter extend. That nicely agrees with the structural analysis of the near-wall region conducted by Sumitani & Kasagi (1995). They showed that near the blowing side the flow is highly populated with small-scale coherent vortical structures, while on the suction side coherent vortical structures appear less frequently, however, at significantly larger scales.

Later in this section new scaling laws will be derived for the present turbulent Poiseuille flow with non-zero blowing and suction ($0.05 < v_0/u_\tau < 0.16$). Already at this point, from the stress distribution displayed in figures 2 and 3, one can predict that at high transpiration rates the near-wall log law does not exist on the suction side because the Reynolds shear stress in that region is negative or equal to zero and that the viscous sublayer at the blowing wall will vanish because viscous stress in the near-blowing-wall region is almost zero.

3.1. *New logarithmic scaling law from Lie symmetries of the correlation equations*

One of the key objectives of the present analysis is to further develop and validate the Lie group theory for the multi-point statistics of turbulence employing the turbulent Poiseuille flow with wall transpiration. The first step to accomplish this objective is to find symmetry transformations which do not change the form of the TPC equation (2.16). The application of these symmetry groups will later facilitate finding a group invariant solution of the TPC equation in fluid mechanics often of self-similar type. Finally, this leads to the reduction of the TPC equation and, at the same time, determines the functional form of the turbulent scaling law for the mean velocity. The final step of the analysis will be the validation of the new turbulent scaling law by employing the present DNS data.

At this point it is important to note that TPC equations (2.12)–(2.16), which are to be analysed with respect to its symmetries, have undergone a large-Reynolds-number asymptotics as was first presented in Oberlack (2000). Therein it is shown that for correlation distances $|r| \leqslant \eta$, where η is the Kolmogorov length scale, all viscous terms in the latter equations vanish. Exclusion of all of the viscous terms from TPC equations (2.12)–(2.16) allows us to recover one scaling symmetry, which was originally lost due to the presence of viscosity.

The starting point of this analysis is the observation that the boundary condition (2.8), in particular for the transpiration velocity, may be symmetry breaking primarily in the core region of the flow. In the present section only an abbreviated approach will be presented, while more mathematical details are available in Oberlack & Rosteck (2010) and in appendix B of Oberlack (2001).

In order to derive a new turbulent scaling law for the present flow from the TPC equation we need to consider the appropriate symmetry transformations. For the

present problem it is sufficient to focus on the three scaling groups ($\bar{T}_1$, $\bar{T}_2$, $\bar{T}'_s$), the translation group in space ($\bar{T}_{x_2}$) and the translation group of the averaged velocity ($\bar{T}_{\bar{U}_i}$). In global form these transformation groups are defined as

$$\bar{T}_1 : t^* = t, \quad \boldsymbol{x}^* = \mathrm{e}^{k_1}\boldsymbol{x}, \quad \boldsymbol{r}^*_{(l)} = \mathrm{e}^{k_1}\boldsymbol{r}_{(l)}, \quad \bar{U}^*_i = \mathrm{e}^{k_1}\bar{U}_i, \quad \bar{P}^* = \mathrm{e}^{2k_1}\bar{P},$$
$$R^*_{ij} = \mathrm{e}^{2k_1}R_{ij}, \quad \overline{pu_j}^* = \mathrm{e}^{3k_1}\overline{pu_j}, \quad \overline{u_ip}^* = \mathrm{e}^{3k_1}\overline{u_ip}, \ldots, \tag{3.2}$$

$$\bar{T}_2 : t^* = \mathrm{e}^{k_2}t, \quad \boldsymbol{x}^* = \boldsymbol{x}, \quad \boldsymbol{r}^*_{(l)} = \boldsymbol{r}_{(l)}, \quad \bar{U}^*_i = \mathrm{e}^{-k_2}\bar{U}_i, \quad \bar{P}^* = \mathrm{e}^{-2k_2}\bar{P},$$
$$R^*_{ij} = \mathrm{e}^{-2k_2}R_{ij}, \quad \overline{pu_j}^* = \mathrm{e}^{-3k_2}\overline{pu_j}, \quad \overline{u_ip}^* = \mathrm{e}^{-3k_2}\overline{u_ip}, \ldots, \tag{3.3}$$

$$\bar{T}'_s : t^* = t, \quad \boldsymbol{x}^* = \boldsymbol{x}, \quad \boldsymbol{r}^*_{(l)} = \boldsymbol{r}_{(l)}, \quad \bar{U}^*_i = \mathrm{e}^{k_s}\bar{U}_i, \quad \bar{P}^* = \mathrm{e}^{k_s}\bar{P},$$
$$R^*_{ij} = \mathrm{e}^{k_s}\left[R_{ij} + \left(1 - \mathrm{e}^{k_s}\right)\bar{U}_i\bar{U}_j\right], \quad \overline{pu_j}^* = \mathrm{e}^{k_s}\overline{pu_j} + (\mathrm{e}^{k_s} - \mathrm{e}^{2k_s})\bar{P}\bar{U}_j,$$
$$\overline{u_ip}^* = \mathrm{e}^{k_s}\overline{u_ip} + (\mathrm{e}^{k_s} - \mathrm{e}^{2k_s})\bar{P}\bar{U}_i, \ldots, \tag{3.4}$$

$$\bar{T}_{x_2} : t^* = t, \quad \boldsymbol{x}^* = \boldsymbol{x} + k_{x_2}, \quad \boldsymbol{r}^*_{(l)} = \boldsymbol{r}_{(l)}, \quad \bar{U}^*_i = \bar{U}_i,$$
$$\bar{P}^* = \bar{P}, \quad R^*_{ij} = R_{ij}, \quad \overline{pu_j}^* = \overline{pu_j}, \quad \overline{u_ip}^* = \overline{u_ip}, \ldots, \tag{3.5}$$

$$\bar{T}_{\bar{U}_i} : t^* = t, \quad \boldsymbol{x}^* = \boldsymbol{x}, \quad \boldsymbol{r}^*_{(l)} = \boldsymbol{r}_{(l)}, \quad \bar{U}^*_i = \bar{U}_i + k_{\bar{U}_i},$$
$$\bar{P}^* = \bar{P}, \quad R^*_{ij} = R_{ij}, \quad \overline{pu_j}^* = \overline{pu_j}, \quad \overline{u_ip}^* = \overline{u_ip}, \ldots. \tag{3.6}$$

Above and also further down, the dots denote the fact that in principle higher-order correlations are part of the symmetry transformation since the full MPC equation is infinite dimensional. This, however, will not be considered presently and we only focus on the mean velocity and the TPC.

The first two scaling symmetries are well known from the Euler and the Navier–Stokes equations describing scaling of space and time. The third one is a rather new group and independent of (3.2) and (3.3). It represents the scaling of all TPC or MPC tensors, and it is a purely statistical property of these equations (Oberlack & Rosteck 2010). In fact, it is a property of all linear equations. One of the most crucial symmetries for the results to follow and also a key ingredient of the classical log law (Oberlack 2001) is symmetry (3.6). It is also of purely statistical nature and was discovered in the context of an infinite set of statistical symmetries in Oberlack & Rosteck (2010). It is noted that the first hint towards (3.6) has been given by Kraichnan (1965).

In local (infinitesimal) form the symmetries (3.2)–(3.6) are given by

$$\bar{X}_1 = x_2\frac{\partial}{\partial x_2} + \bar{U}_i\frac{\partial}{\partial \bar{U}_i} + r_i\frac{\partial}{\partial r_i} + 2R_{ij}\frac{\partial}{\partial R_{ij}} + 3\overline{pu_j}\frac{\partial}{\partial \overline{pu_j}} + 3\overline{u_ip}\frac{\partial}{\partial \overline{u_ip}} + \cdots, \tag{3.7}$$

$$\bar{X}_2 = t\frac{\partial}{\partial t} - \bar{U}_i\frac{\partial}{\partial \bar{U}_i} - 2R_{ij}\frac{\partial}{\partial R_{ij}} - 3\overline{pu_j}\frac{\partial}{\partial \overline{pu_j}} - 3\overline{u_ip}\frac{\partial}{\partial \overline{u_ip}} + \cdots, \tag{3.8}$$

$$\bar{X}_s = \bar{U}_i\frac{\partial}{\partial \bar{U}_i} + (R_{ij} - \bar{U}_i\bar{U}_j)\frac{\partial}{\partial R_{ij}} + \left(\overline{pu_j} - \bar{P}\bar{U}_j\right)\frac{\partial}{\partial \overline{pu_j}} + \left(\overline{u_ip} - \bar{U}_i\bar{P}\right)\frac{\partial}{\partial \overline{u_ip}} + \cdots, \tag{3.9}$$

$$\bar{X}_{x_2} = \frac{\partial}{\partial x_2}, \tag{3.10}$$

$$\bar{X}_{\bar{U}_i} = \frac{\partial}{\partial \bar{U}_i} + \cdots. \tag{3.11}$$

As the latter groups are linearly independent, any linear combination of the symmetries (3.7)–(3.11), yields a new multi-parameter group which is also a symmetry

of the TPC equation. From the latter we may finally construct the invariant surface condition (see e.g. Bluman, Cheviakov & Anco 2010) encompassing all groups given above

$$\frac{\mathrm{d}x_2}{k_1 x_2 + k_{x_2}} = \frac{\mathrm{d}r_{(k)}}{k_1 r_{(k)}} = \frac{\mathrm{d}\bar{U}_i}{(k_1 - k_2 + k_s)\bar{U}_i + k_{\bar{U}_i}} = \cdots, \tag{3.12}$$

where in the present paper any further invariance conditions for higher correlations are omitted.

At this point, none of the group parameters k_i in (3.12) are determined. In order to determine at least some of them we may invoke the condition (2.9), i.e. $\bar{U}_2 = v_0$, as this is the key influencing factor for altering the turbulent Poiseuille flow. As it acts primarily on the velocity we consider the concatenated global transformations for the mean velocity

$$\bar{U}_i^* = \mathrm{e}^{k_1 - k_2 + k_s}\bar{U}_i, \tag{3.13}$$

taken from (3.2)–(3.4) and, for the moment, omit any other part of the transformations. In order to comprehend the following, we may first recall that invariance, and in turn invariant reduction, requires a knowledge of the symmetries admitted by the underlying equation, here the TPC equation (2.16). In a second step, however, for the construction of a concrete solution, symmetries, or a combination of them, have to be consistent to the imposed boundary conditions. Presently this means (3.13) has to be conformal to (2.9) which, after implementing of the former into the latter, leads to

$$\mathrm{e}^{-(k_1 - k_2 + k_s)}\bar{U}_2^* = v_0. \tag{3.14}$$

As the definition of symmetry implies form invariance, also for the boundary conditions, this provides the constraint

$$k_1 - k_2 + k_s = 0. \tag{3.15}$$

We may conclude that the transpiration velocity (v_0) is symmetry breaking, most likely in the core region of the flow but also in the near-wall region.

Imposing the latter constraint onto (3.12) and integrating the first with the third term leads to a new logarithmic scaling law for the streamwise mean velocity in the core region

$$\bar{U}_1 = A_1 \ln\left(\frac{x_2}{h} + B_1\right) + C_1, \tag{3.16}$$

where $A_1 = k_{\bar{U}_1}/k_1$ and $B_1 = k_{x_2}/k_1$ and, hence, they are either functions of the group parameters k_i or simply constants of integration as C_1. If it may be presumed that v_0 is sufficiently large ($0.05 \lesssim v_0^+$) we will subsequently show that the latter new log law is valid in the core region of a turbulent channel flow with wall transpiration.

For the wall-normal component of the mean velocity $\bar{U}_2$ a result similar to (3.16) is obtained from (3.12). Taking into account the additional constraint $k_{\bar{U}_2} = 0$, we obtain $\bar{U}_2(x_2) = C_2$, which nicely confirms using (2.9) that the wall-normal component of mean velocity is a constant and is equal to the transpiration velocity v_0.

3.2. *New viscous sublayer velocity scaling law for the blowing wall*

As was mentioned above, the mean flow momentum equation (2.10) is integrable once leading to (2.11). For a local analysis we may in principle rewrite the momentum equation for each wall and later normalize it on the respective local friction velocities. Presently, however, we will follow a slightly different route and may first reformulate the local friction velocities according to (2.1) and (3.1) by the averaged friction velocity u_τ which is related to the streamwise pressure gradient

$$u_{\tau b}^2 = \frac{a}{h} u_\tau^2, \quad u_{\tau s}^2 = \frac{2h-a}{h} u_\tau^2. \tag{3.17}$$

The coefficients a/h and $(2h - a)/h$ represent the relations τ_{wb}/τ_w and τ_{ws}/τ_w respectively defined by (3.1), where a is a parameter that depends on the transpiration velocity. This facilitates a normalization of the terms of the momentum equation with u_τ rather than with local ones, which allows us to directly compare the scaling of the blowing and the suction wall based on the same scaling. The mean momentum equation (2.11) in integrated form for the blowing side and rewritten in non-dimensional form based on u_τ and ν yields

$$\frac{\mathrm{d}\bar{U}_1^+}{\mathrm{d}x_2^+} - v_0^+ \bar{U}_1^+ - \overline{u_1 u_2}^+ = \frac{a}{h} - \frac{x_2^+}{Re_\tau}. \tag{3.18}$$

Extending the usual universal near-wall region located in the vicinity of the wall where x_2^+ is the wall-normal coordinate and taking the limit $Re_\tau \to \infty$, with $x_2^+ = O(1)$, equation (3.18) reduces to

$$\frac{\mathrm{d}\bar{U}_1^+}{\mathrm{d}x_2^+} - v_0^+ \bar{U}_1^+ - \overline{u_1 u_2}^+ = \frac{a}{h}. \tag{3.19}$$

Finally, for the viscous sublayer at the blowing wall, we take the limit $x_2^+ \to 0$ to obtain $\overline{u_1 u_2}^+ \to 0$ and $v_0^+ \bar{U}_1^+ \to 0$ and hence linear velocity scaling law for the blowing side results

$$\bar{U}_1^+ = \frac{a}{h} x_2^+, \tag{3.20}$$

or in rescaled form

$$\bar{U}_{1b} = x_2^+, \quad \text{where } \bar{U}_{1b} = \frac{\bar{U}_1}{u_{\tau b}} \frac{u_\tau}{u_{\tau b}} = \bar{U}_{1b}^+ u_{\tau b}^+. \tag{3.21}$$

We note that the true local shear stress derives from the prefactor on the right-hand side of (3.20) and may be reformulated to give a local shear stress based scaling law employing (3.17). Since in the classical Poiseuille flow without transpiration the point of zero shear stress coincides with the centreline of the flow, i.e. $a = h$, we observe that the modified scaling law (3.20) recovers the classical one for $v_0 = 0$.

In the presence of the convective momentum transport term $v_0 \bar{U}_1$, the blowing shifts the viscous shear stress away from the wall towards the channel centre as can be taken from figures 2(*d–f*) and 3(*d–f*). Since the viscous stress at the blowing wall is smaller than in a channel with impermeable boundaries, the viscous sublayer at the blowing side is thinner than for the classical flow. At very high transpiration rates

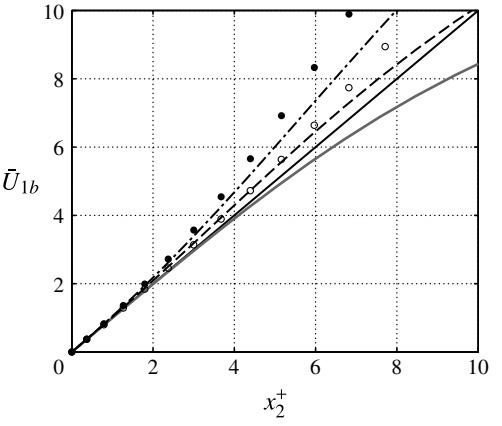

FIGURE 5. Mean velocity profiles and linear law at the blowing wall: —, linear laws (3.20); — , $v_0^+ = 0$; - - -, $v_0^+ = 0.05$; $-\cdot-$, $v_0^+ = 0.1$; ●, $v_0^+ = 0.16$; ○, $v_0^+ = 0.26$.

($v_0/u_\tau = 0.26$), when the local friction velocity becomes smaller than transpiration velocity ($v_0/u_{\tau b} = 2.9$), blowing creates a strong wall-normal flow in the vicinity of the blowing wall, and we see an increased validity of the linear scaling for $\bar{U}_1^+$ as it is obtained in figure 5. However, at such a high transpiration rate the viscous stress at the blowing wall is very small even at high Reynolds numbers, i.e. the streamwise velocity gradient in wall-normal direction is small, as can be taken from figures 2(*f*) and 3(*f*).

3.3. *New viscous sublayer velocity scaling law for the suction wall*

A similar analysis of the viscous sublayer on the suction side is not valid as the flow in that region may not be fully turbulent for large transpiration rates. However, in the limit $\overline{u_1 u_2} \to 0$ it is possible to find the velocity profile by integration of the mean momentum equation (2.10). In its final non-dimensional form the solution may be written as follows

$$\bar{U}_{1s} = \frac{2Re_{v_0}\,\mathrm{e}^{2Re_{v_0}}}{1-\mathrm{e}^{2Re_{v_0}}(1-2Re_{v_0})}\left(1-\mathrm{e}^{-x_{2s}}+\frac{1-\mathrm{e}^{2Re_{v_0}}}{2Re_{v_0}\,\mathrm{e}^{2Re_{v_0}}}x_{2s}\right), \tag{3.22}$$

where dimensionless variables in the near-suction-wall scaling have the following forms:

$$x_{2s} = \frac{x_2 v_0}{\nu}, \quad \bar{U}_{1s} = \frac{\bar{U}_1}{u_{\tau s}}\frac{v_0}{u_{\tau s}} = \bar{U}_{1s}^+ v_{0s}^+, \quad Re_{v_0} = Re_{\tau s} v_{0s}^+ = \frac{h v_0}{\nu}. \tag{3.23}$$

Note that x_{2s} is the wall-normal coordinate, i.e. pointing in a different direction as in the rest of this paper, thus x_{2s} has been replaced by $2Re_{\tau s} - x_{2s}$. Taking the limit $Re_{v_0} \to \infty$, with $x_{2s} = O(1)$, equation (3.22) reduces to the asymptotic suction profile (Griffith & Meredith 1936; Drazin & Riley 2006)

$$\bar{U}_{1s} = 1 - \mathrm{e}^{-x_{2s}}. \tag{3.24}$$

In application to the turbulent wall-bounded flows with suction the near-wall solution (3.24) may have been obtained first by Tennekes (1965). However, due to too

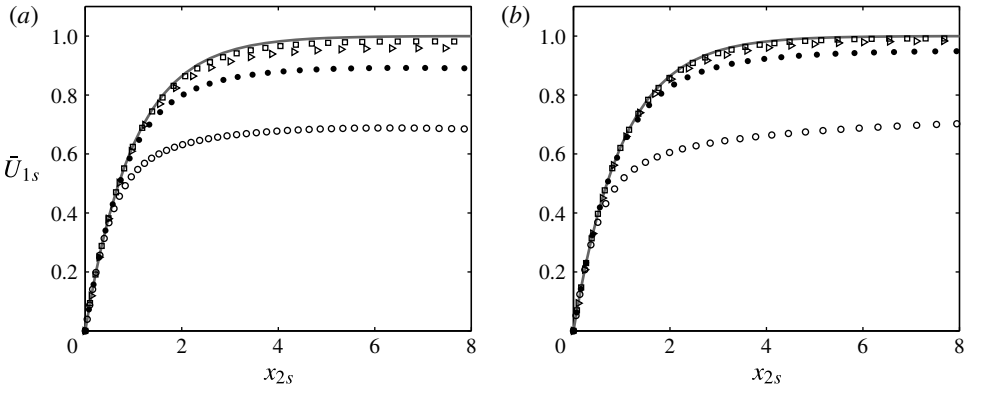

FIGURE 6. Mean velocity profiles and the asymptotic suction profile (3.24) at the suction wall at (*a*) $Re_\tau = 250$ and (*b*) $Re_\tau = 480$: ——, profile (3.24); ○,$v_0^+ = 0.05$; ●, $v_0^+ = 0.10$; △, $v_0^+ = 0.16$; □, $v_0^+ = 0.26$.

wide intervals between velocity traverses in his experiments velocity profiles did not coincide with the analytical solution (3.24). Presently, we verified (3.24) with the DNS, and the results are presented in figure 6(*a*,*b*). As can be taken from figure 6(*a*,*b*), the mean velocity profiles at very high transpiration rates scales with (3.24) much better than at low or moderate transpiration rates. It is also important to note that with increasing Re_τ the domain of agreement between the data and (3.24) increases.

3.4. *Near-wall logarithmic scaling law*

The classical formulation of the near-wall log law traces back to the seminal work of von Kármán (1930). Later Millikan (1939) employed matched asymptotics to express the logarithmic law of the wall as an overlap region. Presently we reconsider a derivation technique based on Lie group analysis, as was used in § 3.1 to find the log law in the core region of the channel flow with wall transpiration.

It was first shown in Oberlack (2001) that the near-wall log law has its roots in Lie symmetries based on a combination of statistical and fluctuating equations. Its first derivation based on the TPC and MPC equations and in particular recognizing the importance of the statistical groups (3.9), (3.11) was obtained in Oberlack & Rosteck (2010). The authors used the infinite set of MPC equations to derive the near-wall log law

$$\bar{U}_1^+ = \frac{1}{\kappa} \ln(x_2^+ + A^+) + C, \tag{3.25}$$

and showed that the friction velocity u_τ is the key symmetry breaking parameter in the near-wall region. The latter is a slightly generalized functional form of the usual near-wall scaling law, as it implies the offset A^+ as a displacement height which gives an extended fit of (3.25) to the experimental data (see e.g. Lindgren, Österlund & Johansson 2004) and further appears, for example, in the log law for rough-wall-bounded flows (Jackson 1981), in the overlap formulation for the turbulent channel and pipe flows proposed by Wosnik, Castillo & George (2000). Recently, similar formulation of the near-wall log law has been identified by Fife, Klewicki & Wei (2009) (also see Klewicki 2013).

An apparent question arises of how (3.25) may change under the influence of the wall transpiration. In the present flow configuration the friction velocity u_τ and the transpiration velocity are of the same dimension and, as shown below, are closely correlated. Further, as both are symmetry breaking for the velocity scaling a functional form of the near-wall log law obtained from Lie group analysis should be similar to the case without transpiration (3.25).

It was shown above that for the viscous sublayers on each wall the local friction velocity is the key normalization parameter in (3.20) and (3.22), as would be naturally expected. This, however, does not appear to be true for the near-wall log law. The collapse of the near-wall data appears to be due to the mean friction velocity u_τ, which is a measure of the pressure gradient. A similar normalization parameter was used by El Telbany & Reynolds (1981), which suggested that an effective friction velocity, i.e. the one that combines the shear stress information on both walls, should be used, and by Wei, Fife & Klewicki (2007), who used a mean friction velocity approach in their analysis of turbulent Couette–Poiseuille flow. This, however, is very different from what was shown in Nikitin & Pavel'ev (1998). They employed a local u_τ on the blowing wall and observed that the usual von Kármán constant κ varies with the blowing velocity.

In order to find the modified constants for the classical near-wall log law in (3.25) due to wall transpiration we may adopt the classical notation given in Millikan (1939). Since blowing increases turbulence it is preferable to derive an unaltered near-wall log law for this region.

According to the results obtained by Jiménez *et al.* (2001) for the channel flow with permeable boundaries, transpiration only affects the additive constant C of the log law, while von Kármán constant κ is largely unaltered in the logarithmic region if a global u_τ is used. As will be shown below, the present DNS seem to support the latter finding and (3.25) may be rewritten in the following form

$$\bar{U}_1^+ = \frac{1}{\kappa}\ln(x_2^+ + A^+) + C + C_1\left(\frac{v_0}{u_\tau}\right), \tag{3.26}$$

keeping in mind how it was normalized and the function C_1 vanishes for vanishing v_0. Here κ and C are independent of v_0 and hence are universal constants obtained for the case without transpiration and based on the global u_τ.

As no first principle idea is known to determine $C_1(v_0/u_\tau)$ we employ a simple curve fitting procedure to fit the new additive function C_1 which comes down to the following power law

$$C_1(v_0^+) = \alpha\left(\frac{v_0}{u_\tau}\right)^\beta, \tag{3.27}$$

where $\alpha = -90.62$ and $\beta = 1.188$.

The results from the DNS and the modified log law calculated from (3.26) with $A^+ = 0$ are compared in figure 7. We observe that the near-wall log law appears to be valid only in the near-wall region on the blowing side, where transpiration increase the Reynolds stress. It was found that the log region is formed only at small ($v_0^+ < 0.1$) transpiration numbers, while at high transpiration rates ($v_0^+ \geqslant 0.16$) it seems to disappear. An indicator function shown on figure 9(*e*, *f*) gives a weak hint toward this conclusion and further confirms the known result that the von Kármán constant κ is very sensitive to the Reynolds number and a flat region is almost invisible for small

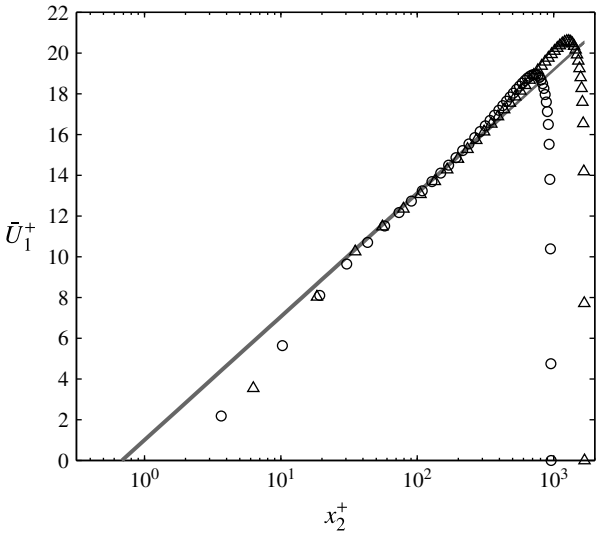

FIGURE 7. Mean velocity profiles of a turbulent channel flow with wall transpiration at the blowing wall. Solid grey line —— corresponds to the log law (3.26), where $\kappa = 0.38$, $A^+ = 0$. Symbols: ○, $Re_\tau = 480$; △, $Re_\tau = 850$.

Reynolds numbers. Presently it is difficult to make any estimates about the near-wall log law scaling region and the value of the von Kármán constant as much higher-Reynolds-number simulations are required.

4. New logarithmic scaling law of the channel centre

The scaling law (3.16) obtained using Lie symmetry method contains constants A_1, B_1 and C_1, that cannot be obtained using Lie group analysis alone. For this reason one of the main aim of the present study is to determine the constants employing the DNS results. An open question that arises immediately is a desired velocity scale, that will induce a collapse of the data in the considered region. Form invariance property of the symmetries has proven previously the assumption that transpiration velocity v_0 is a symmetry breaking constraint in the core region of the flow.

From this one may expect that v_0 is the appropriate velocity scale for the core region log law (3.16). However, a changing of v_0/U_B also significantly changes u_τ/U_B as can be taken from figure 8, and hence the proper velocity scale is not obvious in the first place. From dimensional reasons, the ratio of two velocities result in two non-dimensional groups with a unique functional relation

$$\frac{u_\tau}{U_B} = F\left(\frac{v_0}{U_B}\right). \tag{4.1}$$

The best fit to all DNS data is obtained if instead of v_0 we invoke u_τ as the appropriate velocity scale. We recall that u_τ is a measure of the pressure gradient as the local $u_{\tau b}$ and $u_{\tau s}$ on each wall are very different. The analysis of the DNS results together with the employment of u_τ as a scaling velocity for A_1 leads to the fact that the overall scaling appears rather insensitive to the Reynolds numbers and the relative transpiration rates. The latter rescaling leads to $A_1 = u_\tau/\gamma$, where $\gamma = 0.3$ has been taken from the DNS data. Note that this is not the usual von Kármán constant κ.

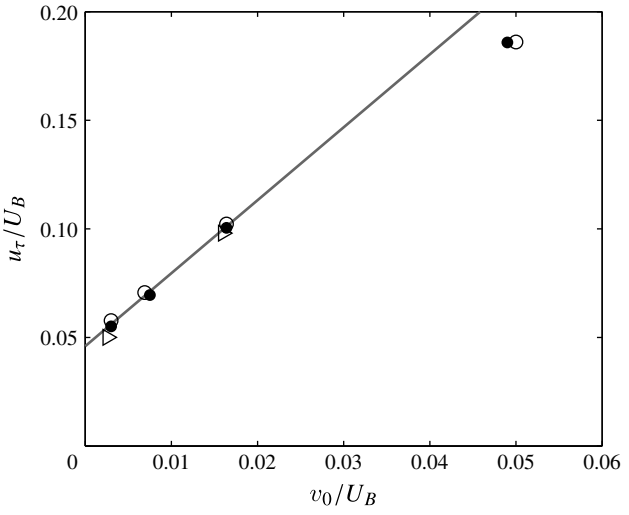

FIGURE 8. Relation between transpiration velocity and friction velocity. Here ○, $Re_\tau = 250$; ●, $Re_\tau = 480$; ▷, $Re_\tau = 850$; —— linear relation between v_0 and u_τ, i.e. $u_\tau = 3.36v_0 + 0.046$.

The offset B_1 in (3.16) was found to be a very small number. Further, a systematic and careful analysis of the best fitted values did not reveal a unique picture. Hence, B_1 has been set to zero for all cases, although a better fit of the DNS data to (3.16) may be obtained from a non-zero B_1.

Since the new log law is located in the centre of the channel, our present knowledge of turbulent scaling laws suggests a defect type of scaling. Hence, a second global velocity scale is needed to determine C_1.

In turbulent boundary-layer flows we use the free-stream velocity U_∞ while in the classical Poiseuille flow U_{max} located in the centre of the channel is the appropriate outer velocity scale. An analysis of the present DNS data disclosed C_1 to be the bulk velocity U_B (2.4) without an additional non-dimensional prefactor.

In its final form the new logarithmic scaling law for the core region of the channel flow with wall transpiration is found to be

$$\bar{U}_1 = \frac{1}{\gamma} u_\tau \ln\left(\frac{x_2}{h}\right) + U_B \tag{4.2}$$

or in deficit form

$$\frac{\bar{U}_1 - U_B}{u_\tau} = \frac{1}{\gamma} \ln\left(\frac{x_2}{h}\right). \tag{4.3}$$

The new Lie-symmetry-induced scaling law (4.3) represents the velocity defect law that scales the data in the whole core region of the flow as may be taken from figure 9. This comparatively long log region already appears at the low Reynolds numbers of $Re_\tau = 250$ and becomes even longer as the Reynolds number is increased to $Re_\tau = 850$ as obtained in figure 9(*c*,*d*). Most important, and as to be expected, the validity of (4.3) further increases with growing transpiration rate v_0, as it is shown in figure 9(*a*,*b*), until the latter becomes only an order of magnitude smaller than the streamwise velocity.

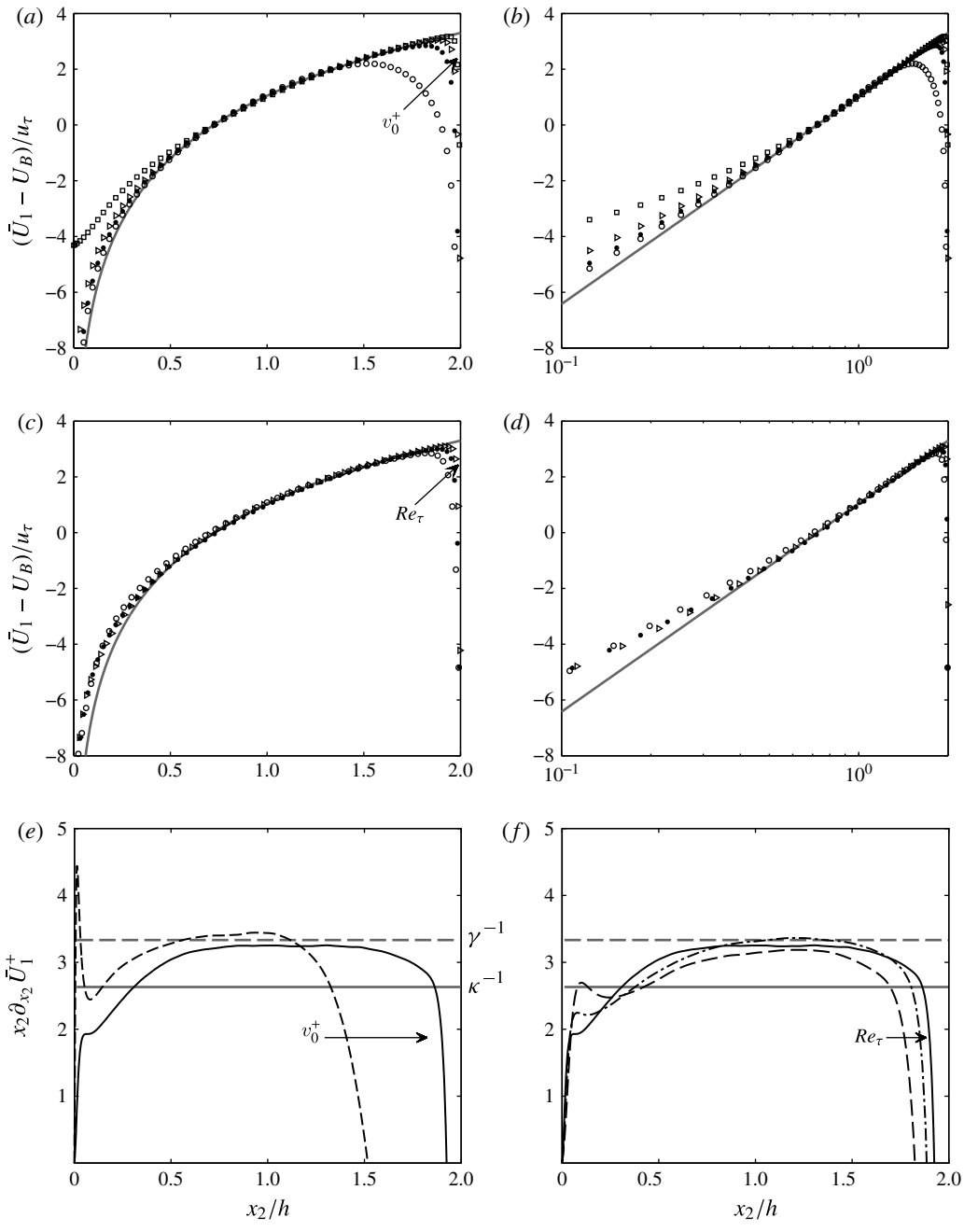

FIGURE 9. Mean velocity profiles at (*a*,*b*) constant Reynolds number $Re_\tau = 480$: ○, $v_0^+ = 0.05$; ●, $v_0^+ = 0.1$; ▷, $v_0^+ = 0.16$; □, $v_0^+ = 0.26$; and (*c*,*d*) constant transpiration rate $v_0^+ = 0.16$: ○, $Re_\tau = 250$; ●, $Re_\tau = 480$; ▷, $Re_\tau = 850$. (*e*, *f*) Indicator function $x_2\partial_{x_2}\bar{U}_1^+$. Grey lines represent slope constants used in the paper. For near-wall region: —, $\kappa = 0.38$; for core region: - - -, $\gamma = 0.3$. (*e*) Constant Reynolds number $Re_\tau = 850$: in direction of an arrow: - - -, $v_0^+ = 0.05$; —, $v_0^+ = 0.16$. (*f*) Constant transpiration rate $v_0^+ = 0.16$: in direction of an arrow: - - -, $Re_\tau = 250$; — -, $Re_\tau = 480$; —, $Re_\tau = 850$.

An indicator function shown in figure 9(*e*,*f*) confirms once again that the new mean velocity scaling law (4.3) is valid in the whole core region of the flow. In particular, it is found that the indicator function has a plateau in the core region, and the slope constant for the new core region log law was found to be $\gamma = 0.3$, as it is highlighted with a dashed line on figure 9(*e*,*f*). Further, the indicator function plot supports the fact that the scaling region of the new mean velocity scaling law increases with Reynolds numbers and moderate (up to $v_0^+ \leqslant 0.16$) transpiration numbers.

5. Discussion and conclusions

In the present paper we combined Lie symmetry analysis of the TPC equations and DNS to investigate the statistical characteristics of the turbulent channel flow with wall transpiration. Lie symmetry analysis revealed a new mean velocity logarithmic type of scaling law that, afterwards, has been confirmed in the centre of the channel and studied in detail by DNS. For the derivation of the new log law we used symmetry transformations which have been previously derived in the TPC and MPC equations (Oberlack 2001; Oberlack & Rosteck 2010). Although the completeness of the set of symmetry groups for turbulence statistics for the MPC equations has not been proven yet, it was sufficient to derive the new scaling law for the core region.

By using the new results from the DNS data it was found, that the slope constant (γ) of the new log law is different from the von Kármán constant and that its value is $\gamma = 0.3$. The presence of the transpiration makes the log region much longer than that of the velocity defect law for the classical channel flow. The new scaling law covers from 65 to 80 % of the channel height depending on the transpiration rate. We observed an increase of the new log law scaling region with increasing transpiration rate, although no first principles theory may be given for this behaviour. The theory does not provide any estimates of the location of the log law. It might be possible to give an estimate for the validity such as the classical one for near-wall log, but we did not observe any clear behaviour and hence decided to avoid unvalidated speculations.

We found weak indications that the classical near-wall scaling laws, i.e. the linear law in the viscous sublayer and logarithmic law of the wall, may still exist on the blowing side although in slightly modified form. Further, we have found that at the suction wall the flow tends to relaminarize and at very high transpiration rates it becomes similar to the asymptotic suction velocity profile in exponential form, as it may be taken from figure 6(*a*,*b*). This indicates that the permeability of the channel walls strongly affects and, in fact, dominates the near-wall region and in particular the wall shear stress. This conclusion in a certain sense is not new, however, results obtained in the present paper show that at very high transpiration rates the properties of the near-wall region are completely changed, that can be taken from figures 2(*f*), 3(*f*) and figure 6(*a*,*b*). We showed that the convective momentum transport $v_0 \bar{U}_1$ exceeds both viscous and Reynolds stresses at the blowing wall and at the same time leads to an almost zero Reynolds stress at the suction wall. From the same figures and also from the fact that the new scaling law (4.3) was successfully validated with DNS data for moderate transpiration rates we may assume that the strong transpiration has also influence on the core region of the flow.

The importance of the present contribution may be contemplated in a somewhat larger context as another brick in the turbulence theory based on Lie symmetries applied to the MPC equation the reason being twofold. First, before the entire project started and before any DNS was conducted the new log scaling laws was forecasted from pure theoretical grounds. Second, the basis for the new log law is partially

based on two of the new statistical groups which have no direct counterpart in the Euler and Navier–Stokes equations for the instantaneous velocities and hence have yet been proven once again to be crucial for our general understanding of the statistics of turbulence.

Acknowledgements

This work was supported by the DFG under the grant number KH 257/2-1 (2010). The computations were performed on the HHLR IBM Regatta supercomputer at TU Darmstadt, on the FUCHS cluster at the University of Frankfurt-am-Main and on the SuperMUC Petascale System at Leibniz Supercomputing Centre (LRZ). Special thanks are due to M. Rampp for providing us an account on the HP Visualization Cluster at the Rechenzentrum Garching (RZG) of the Max Planck Institute for Plasmaphysics (IPP) were we performed visualizations of the data. Finally, the authors would like to thank Y. Wang, M. Frewer and A. Rosteck for their valuable comments.

REFERENCES

ANTONIA, R. S., KRISHNAMOORTHY, L. V., FULACHIER, L., ANSELMET, F. & BENABID, T. 1986 Influence of wall suction on coherent structures in a turbulent boundary layer. In *9th Australasian Fluid Mechanics Conference, Auckland, Australia*, pp. 346–349.

AVSARKISOV, V. S., OBERLACK, M. & KHUJADZE, G. 2011 Turbulent Poiseuille flow with wall-transpiration: analytical study and direct numerical simulation. *J. Phys.: Conf. Ser.* **318**, 022004.

BLACK, T. J. & SARNECKI, A. J. 1958 The turbulent boundary layer with suction or injection. *Tech. Rep. 20*, Cambrige University, Engineering Department.

BLUMAN, G. W., CHEVIAKOV, A. F. & ANCO, S. C. 2010 *Application of Symmetry Methods to Partial Differential Equations*. Springer.

CHUNG, Y. M. & SUNG, H. J. 2001 Initial relaxation of spatially evolving turbulent channel flow with blowing and suction. *AIAA J.* **39** (11), 2091–2099.

CHUNG, Y. M., SUNG, H. J. & KROGSTAD, P.-A. 2002 Modulation of near-wall turbulence structure with wall blowing and suction. *AIAA J.* **40** (8), 1529–1535.

DEL ÁLAMO, J. C. & JIMÉNEZ, J. 2003 Spectra of the very large anisotropic scales in turbulent channels. *Phys. Fluids* **15** (6), 41–44.

DEL ÁLAMO, J. C., JIMÉNEZ, J., ZANDONADE, P. & MOSER, R. D. 2004 Scaling of the energy spectra of turbulent channels. *J. Fluid Mech.* **500**, 135–144.

DRAZIN, P. G. & RILEY, N. 2006 *The Navier–Stokes Equations: A Classification of Flows and Exact Solutions*. Cambridge University Press.

EL TELBANY, M. M. M. & REYNOLDS, A. J. 1981 Turbulence in plane channel flows. *J. Fluid Mech.* **111**, 283–318.

FIFE, P., KLEWICKI, J. C. & WEI, T. 2009 Time averaging in turbulence settings may reveal an infinite hierarchy of length scales. *J. Discrete Continuous Dyn. Syst.* **24** (3), 781–807.

GRIFFITH, A. A. & MEREDITH, F. W. 1936 Possible improvement in aircraft performance due to use of boundary layer suction. *Tech. Rep. 2315*, Aero. Res. Counc., London.

HANJALIĆ, K. & LAUNDER, B. E. 1972*a* Fully developed asymmetric flow in a plane channel. *J. Fluid Mech.* **51** (2), 301–335.

HANJALIĆ, K. & LAUNDER, B. E. 1972*b* Reynolds-stress model of turbulence and its application to thin shear flows. *J. Fluid Mech.* **52** (4), 609–638.

HINZE, J. O. 1959 *Turbulence, An Introduction to its Mechanism and Theory*. McGraw-Hill.

HOYAS, S. & JIMÉNEZ, J. 2006 Scaling of the velocity fluctuations in turbulent channels up to $Re_\tau = 2003$. *Phys. Fluids* **18**, 011702.

JACKSON, P. S. 1981 On the displacement height in the logarithmic velocity profile. *J. Fluid Mech.* **111**, 15–25.

JIMÉNEZ, J., UHLMANN, M., PINELLI, M. & KAWAHARA, G. 2001 Turbulent shear flow over active and passive porous surfaces. *J. Fluid Mech.* **442**, 89–117.

JOHNSTONE, R., COLEMAN, G. N. & SPALART, P. R. 2010 The resilience of the logarithmic law to pressure gradients: evidence from direct numerical simulation. *J. Fluid Mech.* **643**, 163–175.

KAMETANI, Y. & FUKAGATA, K. 2011 Direct numerical simulation of spatially developing turbulent boundary layer with uniform blowing or suction. *J. Fluid Mech.* **681**, 154–172.

KELLER, L. & FRIEDMANN, A. 1924 Differentialgleichungen für die turbulente Bewegung einer kompressiblen Flüssigkeit. In *Proc. First. Int. Congr. Appl. Mech.*, pp. 395–405.

KIM, J., MOIN, P. & MOSER, R. 1987 Turbulence statistics in fully developed channel flow at low Reynolds number. *J. Fluid Mech.* **177**, 133–166.

KLEWICKI, J. C. 2013 Self-similar mean dynamics in turbulent wall flows. *J. Fluid Mech.* **718**, 596–612.

KRAICHNAN, R. H. 1965 Lagrangian-history closure approximaiton for turbulence. *Phys. Fluids* **8** (4), 575–598.

LAUNDER, B. E., REECE, G. J. & RODI, W. 1975 Progress in the development of a Reynolds-stress turbulence closure. *J. Fluid Mech.* **68** (3), 537–566.

LELE, S. K. 1992 Compact finite difference schemes with spectral-like resolution. *J. Comput. Phys.* **103**, 16–42.

LINDGREN, B., ÖSTERLUND, J. M. & JOHANSSON, A. V. 2004 Evaluation of scaling laws derived from lie group symmetry methods in zero-pressure-gradient turbulent boundary layers. *J. Fluid Mech.* **502**, 127–152.

MCCOMB, W. D. 1990 *The Physics of Fluid Turbulence*. Oxford University Press.

MICKLEY, H. S. & DAVIS, R. S. 1957 Momentum Transfer for Flow Over a Flat Plate with Blowing. In *Tech. Rep.*, vol. 4017. MIT.

MILLIKAN, C. B. 1939 A critical discussion of turbulent flows in channels and circular tubes. In *Proc. Vth Int. Congr. Appl. Mech.*, pp. 386–392.

NAKABAYASHI, K., KITOH, O. & KATOH, Y. 2004 Similarity laws of velocity profiles and turbulence characteristics of Couette–Poiseuille turbulent flows. *J. Fluid Mech.* **507**, 43–69.

NIKITIN, N. V. & PAVEL'EV, A. A. 1998 Turbulent flow in a channel with permeable walls. DNS and results of three-parameter-model. *J. Fluid Mech.* **33** (6), 826–832.

OBERLACK, M. 2000 Symmetrie, Invarianz und Selbstähnlichkeit in der Turbulenz. Habilitation thesis.

OBERLACK, M. 2001 A unified approach for symmetries in plane parallel turbulent shear flows. *J. Fluid Mech.* **427**, 299–328.

OBERLACK, M. & ROSTECK, A. 2010 New statistical symmetries of the multi-point equations and its importance for turbulent scaling laws. *Discrete Continuous Dyn. Syst.* S **3** (3), 451–471.

ROSTECK, A. & OBERLACK, M. 2011 Lie algebra of the symmetries of the multi-point equations in statistical turbulence theory. *J. Nonlinear Math. Phys.* **18**, 251–264.

SCHLATTER, P. & ÖRLÜ, R. 2011 Turbulent asymptotic suction boundary layers studied by simulation. *J. Phys.: Conf. Ser.* **318**, 1–10.

STEVENSON, T. N. 1963*a* A Law of the Wall for Turbulent Boundary Layers with Suction or Injection. In *Tech. Rep.*, vol. 166. The College of Aeronautics Cranfield.

STEVENSON, T. N. 1963*b* 1963b A modified velocity defect law for turbulent boundary layers with injection. *Tech. Rep.* 170 The College of Aeronautics Cranfield.

SUMITANI, Y. & KASAGI, N. 1995 Direct numerical simulation of turbulent transport with uniform wall injection and suction. *AIAA J.* **33** (7), 1220–1228.

TENNEKES, H. 1965 Similarity laws for turbulent boundary layers with suction or injection. *J. Fluid Mech.* **21** (4), 689–703.

TENNEKES, H. & LUMLEY, J. L. 1972 *A First Course in Turbulence*. The MIT Press.

VIGDOROVICH, I. & OBERLACK, M. 2008 Analytical study of turbulent Poiseuille flow with wall-transpiration. *Phys. Fluids* **20**, 055102.

VON KÁRMÁN, TH. 1930 In *Mechanische Ähnlichkeit und Turbulentz* Nachr. Ges. Wiss. Göettingen, Math-Phys. Kl., vol. 68.

VON KÁRMÁN, TH. & HOWARTH, L. 1938 On the statistical theory of isotropic turbulence. *Proc. R. Soc. Lond.* A **164**, 192–215.

WEI, T., FIFE, P. & KLEWICKI, J. 2007 On scaling the mean momentum balance and its solutions in turbulent Couette–Poiseuille flow. *J. Fluid Mech.* **573**, 371–398.

WOSNIK, M., CASTILLO, L. & GEORGE, W. K. 2000 A theory for turbulent pipe and channel flows. *J. Fluid Mech.* **421**, 115–145.

ZHAPBASBAYEV, U. & ISAKHANOVA, G. 1998 Developed turbulent flow in a plane channel with simultaneous injection through one porous wall and suction through the other. *J. Appl. Mech. Tech. Phys.* **39**, 53–59.